Available online at www.sciencedirect.com

SCIENCE DIRECT®

Optics & Laser Technology 35 (2003) 309–313

Optics & Laser Technology

www.elsevier.com/locate/optlastec

Influence of the UV-induced fiber loss on the distributed feedback fiber lasers☆

Wei Fan*, Bai Chen, Qiquan Qiao, Jialing Chen, Zunqi Lin

National Laboratory of High Power Laser and Physics, Shanghai Institute of Optics and Fine Mechanics, Chinese Academy of Sciences, Box 800-211, Shanghai 201800, China

Received 22 November 2002; received in revised form 9 January 2003; accepted 20 January 2003

Abstract

It was found that the output power of the distributed feedback fiber lasers would be improved after annealing or left unused for several days after the laser had been fabricated, and the output of the fundamental mode would not increase but be clamped while the ±1 order modes would be predominant with the enhancement of the coupling coefficient during the fabrication. The paper discussed the influence of UV-induced fiber loss on the fiber phase-shifted DFB lasers. Due to the gain saturation and fiber internal loss, which included the temperament loss and permanent loss, there was an optimum coupling coefficient for the DFB fiber lasers that the higher internal fiber loss corresponded to the lower optimum values of coupling coefficient.

Keywords: Distributed feedback fiber laser; Fiber loss; Coupling coefficient

1. Introduction

Single frequency, continuous wave fiber lasers are required for a wide range of applications and spectroscopy [1,2]. An efficient and very attractive way to accomplish a single frequency fiber laser is to use distributed feedback (DFB) structure with a $\lambda/4$ phase shift, as is common for semiconductor lasers [3]. And because they are fiber compatible, have extremely narrow linewidth, can provide high output powers, and foremost, can be easily made with accurate and predefined wavelengths, the fiber lasers have definite advantage over conventional semiconductor sources.

The phase-shifted DFB fiber lasers were fabricated by UV illuminating the active fiber. In order to increase the photosensitivity, the fiber was hydrogenated for more than 1 week at the normal temperature.

It was found that the output power would increase and the threshold would decrease if the fiber DFB lasers were left unused for several days or annealing at high temperature for several hours after the fabrication. During the fabrication, the fundamental mode would not increase but be clamped while the ±1 order modes would be predominant with the enhancement of the coupling coefficient. The references [4,5] denoted that the internal fiber loss would increase if the fiber was hydrogenated and with the diffuse of the hydrogen, the internal loss would be relaxed. But if the hydrogenated fiber had been UV exposed, there would be some permanent loss left. The paper discussed the influence of the fiber internal loss on the phase-shifted DFB fiber lasers. The corresponding experimental phenomena were given.

2. Numerical simulations

2.1. Theory

The Yb^{3+} energy level structure consists of two manifolds, the ground manifold $^2F_{7/2}$ with four stark levels and a separated excited manifold $^2F_{5/2}$ with three stark levels. For convenience, one can use a quasi-two-level description [6]

$$\frac{\partial N_2}{\partial t} = -\frac{\partial N_1}{\partial t} = -\frac{N_2}{T_1} + \left[\frac{\sigma_{as}}{S_s\hbar\omega_s}|E|^2 + \frac{\sigma_{ap}}{S_p\hbar\omega_p}P_p\right]N_1 - \left[\frac{\sigma_{es}}{S_s\hbar\omega_s}|E|^2 + \frac{\sigma_{ep}}{S_p\hbar\omega_p}P_p\right]N_2. \quad (1)$$

☆ The work is supported by National Hi-Tech 863 Foundation of China.
* Corresponding author. Fax: +86-21-6991-8800.
E-mail addresses: fanweil@siom.ac.cn, lfanwei@hotmail.com (W. Fan).

0030-3992/03/$ - see front matter
doi:10.1016/S0030-3992(03)00025-2

Here T_1 is the spontaneous decay time, ω_p and ω_s are the frequency of the pump wave and signal wave respectively, P_p is the pump power, S_p and S_s are the effective area of the pump mode and signal mode respectively, $E=E_+\exp(i\beta z)+E_-\exp(-i\beta z)$ is the total complex amplitude of the lasing field, E_+ and E_- are the forward and backward lasing field respectively, β is the propagation constant, σ_{as}, σ_{es}, σ_{ap}, σ_{ep} denote the absorption, emission cross-section of the signal wavelength, and the pump wavelength, respectively. N_1 and N_2 are the populations of the upper and lower laser levels, respectively, $N_1+N_2=N_0$, where N_0 is the concentration of active ions in the host material. For steady-state operation of the device far enough above threshold for the spontaneous emission to be neglected, the gain $g=(S_i/S_s)[\sigma_{es}N_2-\sigma_{as}N_1]$, where S_i is the area of the transverse distribution of active ions, can be expressed in the following form [6]:

$$g=\frac{g_0}{1+(\omega_p/\omega_s)(g_0/\alpha_0P_p)[E_+\exp(i\beta z)+E_-\exp(-i\beta z)]^2}. \quad (2)$$

The unsaturated gain at full inversion is

$$g_0=N_0\frac{S_i}{S_s}\frac{\sigma_{es}\sigma_{ap}-\sigma_{ep}\sigma_{as}}{\sigma_{ap}+\sigma_{ep}} \quad (3)$$

and the coefficient of small signal resonant absorption in an unpumped medium is

$$\alpha_0=N_0\frac{S_i}{S_p}\frac{\sigma_{es}\sigma_{ap}-\sigma_{ep}\sigma_{as}}{\sigma_{as}+\sigma_{es}}. \quad (4)$$

The absorption and dispersion may influence the inversion population of the active ions, so the pump power depletion along the fiber must be taken account. The following equation is used to describe the pump power distribution in the longitudinal direction of the fiber:

$$\frac{dP_p(z)}{dz}=\frac{S_i}{S_p}(\sigma_{ep}N_2-\sigma_{ap}N_1-\alpha_L)P_p(z), \quad (5)$$

where α_L stands for the internal fiber loss.

Taking the fiber internal loss into account, the pure gain per unit length was $g_p=g-\alpha_L$. For convenience, it was supposed that the magnitude of fiber internal loss is the same for the pump wavelength and signal wavelength.

The effects of the grating are treated using the coupled mode theory and included in the numerical simulation through the use of the transmission matrix model described in Refs. [7,8].

Considering a section of the fiber grating, of which the length is Δz and the internal gain is g, the transmission matrix can be expressed as [7]

$$\begin{pmatrix} E_A(z+\Delta z) \\ E_B(z+\Delta z) \end{pmatrix}=[F]\begin{pmatrix} E_A(z) \\ E_B(z) \end{pmatrix}. \quad (6)$$

The elements of F matrix in Eq. (6) are given as follows:

$$F_{11}=[\cosh(\gamma\Delta z)-i\Delta\beta' L\sinh(\gamma\Delta z)/(\gamma L)]\exp(-i\beta\Delta z),$$
$$F_{12}=ikL\sinh(\gamma\Delta z)\exp(-i(\Delta\beta\Delta z+\phi)]/(\gamma L),$$
$$F_{21}=ikL\sinh(\gamma\Delta z)\exp(i(\Delta\beta\Delta z+\phi)]/(\gamma L),$$
$$F_{22}=[\cosh(\gamma\Delta z)+i\Delta\beta' L\sinh(\gamma\Delta z)/(\gamma\Delta z)]\exp(i\Delta\beta\Delta z).$$

Here,

$$\Delta\beta L'=\Delta\beta L+igL,$$

$$(\gamma L)^2=(kL)^2-(\Delta\beta' L)^2,$$

$$\Delta\beta=\beta-\beta_B=\beta-M\pi/\Lambda,$$

kL is the coupling coefficient of the grating. Λ is the grating period. Since, we are concerned with the first order of the grating, namely, $M=1$. The F matrix satisfies the reciprocity, that is, the determinant of the matrix is unity, namely,

$$|F|=F_{11}F_{22}-F_{12}F_{21}.$$

Applying boundary conditions, one arrives at

$$E_A(0)=1,$$

$$E_B(L)=0. \quad (7)$$

The fiber grating was divided into $N=301$ sections, $L=\sum_{j=1}^{N}\delta l_j$. The phase relation at the interface between the $(j-1)$th and jth segments is given by $\phi_j=\phi_{j-1}+2\beta_B\delta l_{j-1}+\Delta\phi$.$\Delta\phi$ is the magnitude of phase shift.

$$\Delta\phi=\begin{cases}\pi\left(j=\dfrac{N-1}{2}\right),\\ 0\left(j\neq\dfrac{N-1}{2}\right).\end{cases} \quad (8)$$

The calculation start from the left end with signal wavelength and a forward propagating pump power. Then evaluate the transfer matrix and propagate the field through the first section. In the next step, we expose the next grating section with the output from the first section. This procedure is continued until we reach the right end of the grating, the magnitude of the out-going signal $E_B(0)$ are adjusted until the boundary condition $E_B(L)=0$ is fulfilled.

2.2. Modeling results

The parameters we used in the computations are summarized in Table 1:

First, the influence of the fiber internal loss from 2 to 0.0001 dB/m on the output power of the phase-shifted DFB fiber lasers with coupling coefficient $kL=4.5, 6, 8, 10$

Table 1
Summary of parameters used in the computations

Parameters		Parameters	
Pump wavelength (λ_p)	980 nm	Absorb cross-section (σ_{ap}) Emission cross-section (σ_{ep})	600×10^{-27} m^2 600×10^{-27} m^2
Signal wavelength (λ_s)	1053 nm	Absorb cross-section (σ_{as}) Emission cross-section (σ_{es})	15×10^{-27} m^2 420×10^{-27} m^2
Pump power (p_p)	50 mW	Effective refractive index (n_{eff})	1.47
Length of the grating (L)	10 cm	Concentration of active ions (N_0)	1.92×10^{25} m^{-3}
S_i/S_s	0.75	S_i/S_p	0.8

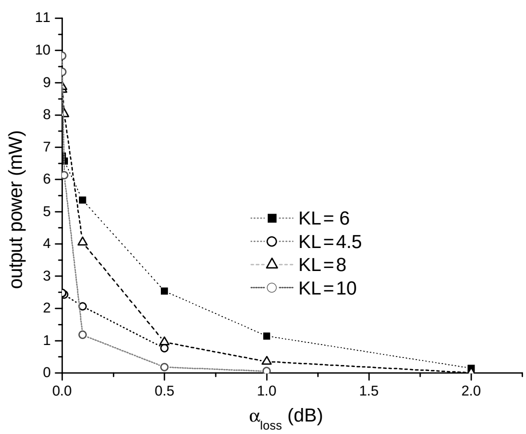

Fig. 1. Output power versus fiber internal loss with different coupling coefficient $kL(p_p = 50$ mW).

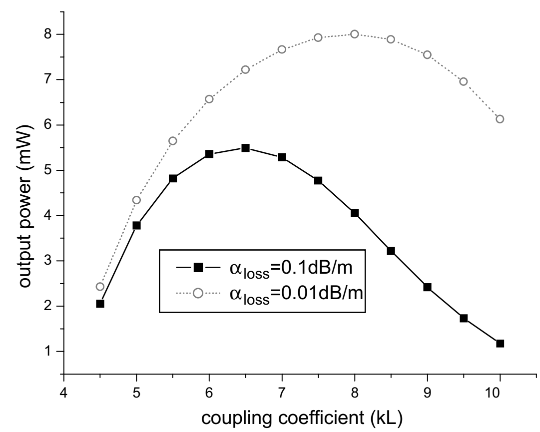

Fig. 2. Output power versus coupling coefficient with different fiber internal loss ($p_p = 50$ mW).

was calculated and illustrated in Fig. 1. For the standard single-mode fiber, the fiber loss is 0.0002–0.0004 dB/m, which would be increased after hydrogenation and UV exposure [4,5].

From Fig. 1, it can be seen that with the increase of the fiber internal loss, the output power decreased. The larger the coupling coefficient, the greater influence on the output power of the lasers.

Fig. 2 is the demonstration of output power versus the coupling coefficient with fiber internal loss 0.1 and 0.01 dB/m. It is easy to see that there is an optimum coupling coefficient value for the maximum output power. And the higher the fiber loss, the smaller the range of the optimum coupling coefficient values to obtain high output power.

In order to understand the reason for the great influence of the fiber loss on the phase-shifted DFB fiber lasers with strong coupling coefficient, we calculated the distribution of the gain along the fiber grating with the fiber internal loss 0.1 dB/m and the coupling coefficient 4.5,6,8 illustrated as Fig. 3. From Fig. 3, one can see that the larger the coupling coefficient, the more distinct of the gain saturation is at the center of the fiber grating. Indeed, for phase-shifted DFB lasers, the signal intensity focuses on the phase-shifted region [8], where the population inversion depletion will be highest and the gain at the phase-shifted region more likely to saturate. For the pure gain $g_g = g - \alpha_L$, the fiber loss has greater influence on the small gain along the fiber.

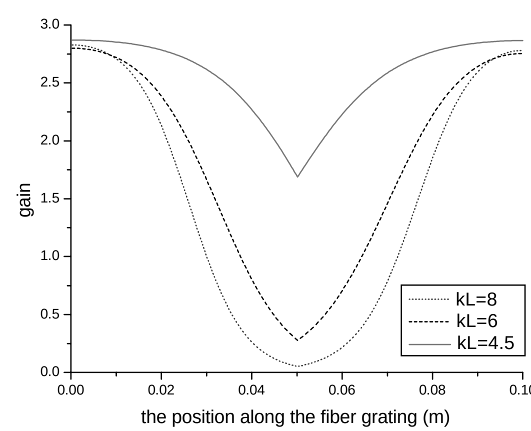

Fig. 3. The gain distribution along the fiber grating with different coupling coefficient $kL(p_p = 50$ mW).

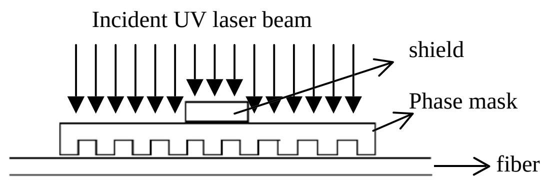

Fig. 4. Experimental setup using the shielded method for fabricating the phase-shifted grating.

3. Experimental work

The phase-shifted DFB fiber lasers were fabricated by shielded method. As illustrated in Fig. 4, the UV light transmitted the phase mask, exposure along the 10 cm length of the Yb^{3+} doped fiber. During the exposure, a section of the fiber was shielded at the center of the light route before it arrived at the phase mask. The fiber had been left into the 150 atm pressure chamber for 2 weeks at room temperature for hydrogen loading. The transmission spectrum and the output were monitored during the fabrication.

The diameter of the fiber core is 6.10 μm, the cut-off wavelength is 907 μm, the absorption at 975 nm is 68 dB/m.

Through the following phenomena, it can be found that the UV-induced fiber loss may play an important role.

Phenomenon I: The hydrogenated Yb^{3+}-doped fiber was exposed under UV light through a phase mask. During the exposure, the 10 mm long was shielded at the center of the light route. The energy of the UV laser is 26 mJ. The repetition rate is 3 Hz. As soon as the reflectivity reached 17.2 dB (98.09%), the laser began to lase at the Bragg wavelength 1053.04 nm and an output power of −38.4 dB m was recorded by an optical spectrum analyzer. Further UV-exposure led to two successive cycles of extinction and restoration of the laser action before definitive emission extinction. The first laser emission reappearance was at 1053.232 nm and with lower output power than the first time while the second showed dual wavelength operation at 1053.384 and 1053.456 nm and with even lower output power. The observed behaviors can be explained as follows. First, when the phase-shifted magnitude reached $\lambda/4$, the fundamental mode was excited and led to the initial laser action. As the fiber continued to be exposed, the central phase shift deviated from $\lambda/4$ causing a threshold increase hence a reduction in the output power. When the central phase shift reached the next $\lambda/4$ shift, the first laser reappearance occurred. Even though the coupling coefficient had been enhanced, the output power decreased. Based on previous calculations, it is thought that the additional UV-exposure led to an increase in the fiber internal loss. The dependence of the output power on the coupling strength was enhanced as shown in Fig. 1 but acted detrimentally in that case. Finally, the second laser restoration also occurred when the phase shift corresponded to a multiple of $\lambda/4$. The dual wavelength operation originated in the fact that the fundamental mode was clamped while the higher order modes used the remaining of the population inversion to reach threshold and above.

Phenomenon II: Then we fabricated another 10 cm DFB fiber laser, of which the phase-shifted region is 10 mm. The energy of the UV laser is 24 mJ. The repetition rate is 2 Hz. As soon as the reflectivity of the fiber grating reached 28.2 dB while the center wavelength is 1053.184 nm, the UV exposure was stopped. But now the DFB fiber laser has no laser output. After annealing for 3 h at the temperature 150°C, the output power is 317 μW at the same pump power 120 mW. The center wavelength moved to 1052.964 nm, which is also the signal wavelength.

Phenomenon III: We fabricated the third DFB fiber lasers, of which the phase-shifted region is 800 μm. During the fabrication, the energy of the UV laser was 24 mJ. The repetition rate is 2 Hz. When the reflectivity is 27.88 dB and the center wavelength of the grating is 1053.208 nm, the UV exposure was stopped. At this time, there is no laser output. But after left unused for 15 days, it can output 74 μW at the same pump power 120 mW. The center wavelength also moved to shorter wavelength.

For the phenomenon II and III, it was considered that due to hydrogenation and UV exposure, the internal fiber loss would increase, which resulted in the increase of the threshold. Left the fiber grating unused for several days or annealed at the high temperature, the hydrogen, which had not taken part in the reactivity, would diffuse. Then the internal loss decreased, which resulted in the decrease of the threshold and increase of the output power. The center wavelength of the grating moved to shorter wavelength implied that the effective index had decreased with the diffusion of the hydrogen.

4. Conclusion

The paper discussed the influence of the fiber internal loss on the fiber DFB lasers. From the experimental phenomena, it was found that the output power of the DFB fiber lasers would be improved after annealing or left unused for several days after the laser had been fabricated and the output of the fundamental mode would not increase but be clamped while the ±1 order modes would be predominant with the enhancement of the coupling coefficient during the fabrication. Through the theoretical analysis and the experimental result, we get the conclusion that the phenomena was due to the fiber internal loss which was induced by the hydrogenation and UV exposure. And due to the gain saturation and fiber internal loss, there was an optimum coupling coefficient for the DFB fiber lasers that the higher internal fiber loss corresponded to the lower optimum values of coupling coefficient.

References

[1] Cheng Y, Kringlebotn JT, Loh WH, et al. Stable single-frequency traveling-wave fibre loop laser with integral saturable-absorber-based tracking narrow-band filter. Opt Lett 1995;20(4): 875–7.

[2] Zyskind JL, Mizrahi V, et al. Short single frequency Erbium-doped fiber laser. Electron Lett 1992;28(15):1385–7.

[3] Asseh A, Storoy H, et al. 10 cm Yb DFB fiber laser with permanent phase shifted grating. Electron Lett 1995;31(12):969–70.

[4] Atkins RM, Lemaire PJ. Effects of elevated temperature on hydrogen exposure on short wavelength optical loss and defect concentration in German-osilicate optical fibers. J Appl Phys 1992; 72(2):344–8.

[5] Stone J. Interactions of hydrogen and deuterium with silica optical fibers: a review. J Lightwave Technol 1987;5(5):712–33.

[6] Jaskorzynska B, Vanin EV, et al. Gain saturation and pump depletion in high-efficiency distributed-feedback rare-earth-doped lasers. Opt Lett 1996;21(17):1366–8.

[7] Yamadam M, Sakuda K. Analysis of almost-periodic distributed feedback slab waveguide via a fundamental matrix approach. Appl Opt 1987; 26(16):3474–8.

[8] Lauridsen VC, Sondegraard T, Varming P. et al. Design of distributed feedback fiber lasers. Ecoc97, 1997. p. 39–42.